Frequency- and Notch-Depth-Tunable Single-Notch Microwave Photonic Filter

Enming Xu and Jianping Yao, *Fellow, IEEE*

***Abstract*— A single-notch microwave photonic filter with tunable frequency and tunable notch depth is proposed and experimentally demonstrated. In the proposed filter, two phase-modulated optical signals at two different wavelengths are generated at a phase modulator. One phase-modulated signal is filtered by a phase-shifted fiber Bragg grating with an ultra-narrow notch to remove the upper sideband. The other phase-modulated signal is filtered by a wideband optical bandpass filter to remove the lower sideband. Since the remaining lower and upper sidebands in the two optical signals are out of phase, the combination of the beat signals at a photodetector will lead to the cancelation of the detected microwave signals, to generate an ultranarrow notch. An experiment is performed. A single-notch microwave photonic filter with a 3-dB bandwidth of ∼180 MHz, a tunable frequency from 1.5 to 6.6 GHz, and a tunable notch depth from 0 to 42 dB is experimentally demonstrated.**

***Index Terms*— Microwave filters, microwave photonics, notch filters, phase-shifted fiber Bragg grating (PS-FBG).**

I. Introduction

PROCESSING of microwave signals in the optical domain has been a topic of interest in the last two decades. The key advantages offered by photonics include low loss, broadband width, and large tunability [1], [2]. Among the numerous signal processing functions, frequency-tunable notch filtering is an important function which can find applications in radar, warfare and wireless communications systems to mitigate jamming signals [3], [4].

A microwave photonic notch filter can be implemented based on a multi-tap delay-line filter with a finite impulse response (FIR). The taps can be realized using a sliced broadband light source or a laser array [5]–[7]. The tuning of the center frequency is usually performed by tuning the wavelength spacing, which is very complicated and costly. A microwave photonic notch filter can also be implemented based on a delay-line filter with an infinite impulse response (IIR) [8]–[10], but the implementation is more complicated, especially the stability is poorer due to the feedback nature of an IIR configuration. In addition, for a microwave photonic notch filter with either an FIR or an IIR, due to the discrete nature of the sampling process in the time domain, the spectral response is periodic. If the time delay difference between two adjacent taps is large, which is true for most implementations, especially for implementations based on fiber delay lines, the free spectral range (FSR) is small, which may make the filter have multiple notches within the spectral range of interest. Thus, it is highly demanded to implement a microwave photonic notch filter with only a single notch. Furthermore, for adaptive jamming mitigation, a notch with a tunable central frequency and tunable notch depth is also needed. Recently, microwave photonic filters (MPFs) with a single notch based on stimulated Brillouin scattering (SBS) were proposed [11]–[13]. The basic concept to achieve a single notch is to manipulate the phase and the amplitude of the two optical sidebands, to fully cancel the microwave signals at a specific frequency at the output of a photodetector (PD), to achieve a high rejection ratio. The main limitation of an SBS-based approach is the complexity of the system.

In this letter, we propose a new and simple MPF with a single notch that is both frequency and notch depth tunable. The fundamental concept to generate a notch is to produce two optical single-sideband (SSB) signals with the two sidebands in the two optical signals out of phase. In the proposed filter, two light waves from two laser diodes (LDs) at $\lambda 1$ and $\lambda 2$ are phase modulated at a phase modulator (PM) and then sent to a phase-shifted fiber Bragg grating (PS-FBG) and a wideband optical bandpass filter (OBPF), respectively. The PS-FBG has an ultra-narrow notch which is used to remove the upper sideband of the first phase-modulated signal, thus a single bandpass filter is implemented. The other phase-modulated signal is filtered by the OBPF to remove the lower sideband, thus an allpass filter is implemented. Since the remaining lower and upper sidebands in the two optical signals are out of phase, the combination of the beat signals at a PD will lead to the cancellation of the detected microwave signals, i.e., the spectral responses of the single bandpass filter and the allpass filter are subtracted to achieve a single notch filter. The notch frequency of the MPF can be tuned by adjusting the wavelength of the light wave at $\lambda 1$, and the notch depth can be tuned by changing the power difference between the two wavelengths at $\lambda 1$ and $\lambda 2$. The proposed approach is experimentally evaluated. A single-notch microwave photonic filter with a 3-dB bandwidth of about 180 MHz, a tunable frequency from 1.5 to 6.6 GHz, and a tunable notch depth from 0 to 42 dB is experimentally demonstrated.

II. Operational Principle

The schematic diagram of the proposed frequency- and notch-depth-tunable single-notch MPF is shown in Fig. 1(a).

Manuscript received April 21, 2015; revised June 20, 2015; accepted June 24, 2015. Date of publication June 29, 2015; date of current version August 31, 2015. This work was supported by the Natural Sciences and Engineering Research Council of Canada. The work of E. Xu was supported by the Jiangsu Government Scholarship Program for Overseas Studies.

E. Xu is with the Microwave Photonics Laboratory, School of Electrical Engineering and Computer Science, University of Ottawa, Ottawa, Ontario, K1N 6N5, Canada, and also with the School of Optoelectronic Engineering, Nanjing University of Posts and Telecommunications, Nanjing 210023, China.

J. Yao is with the Microwave Photonics Research Laboratory, School of Electrical Engineering and Computer Science, University of Ottawa, ON K1N 6N5, Canada (e-mail: jpyao@eecs.uottawa.ca).

Color versions of one or more of the figures in this letter are available online at http://ieeexplore.ieee.org.

Digital Object Identifier 10.1109/LPT.2015.2450719

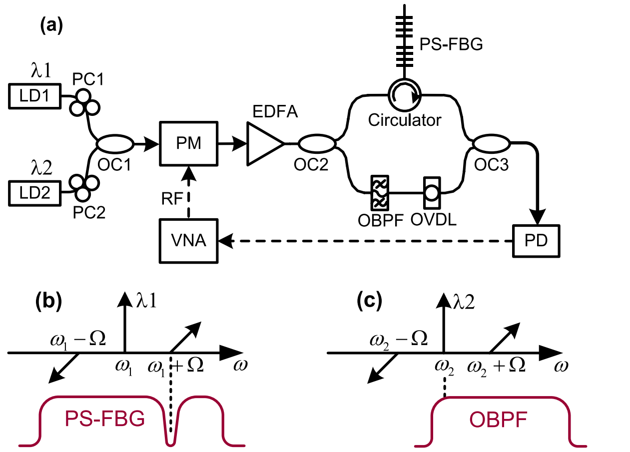

Fig. 1. (a) Schematic of the proposed single-notch MPF. (b) The spectral relationship between the phase-modulated signal and the PS-FBG. (c) The spectral relationship between the phase-modulated signal and the OBPF.

The spectral relationship between the phase-modulated signal and the PS-FBG is shown in Fig. 1(b), and that of the phase-modulated signal and the OBPF is shown in Fig. 1(c). Two light waves from two LDs at $\lambda 1$ and $\lambda 2$ are combined at an optical coupler (OC1) and then sent to a PM. The polarizations of the two light waves are aligned with the principal axis of the PM by using two polarization controllers (PC1 and PC2) to minimize the polarization-dependent loss. The phase-modulated signals at $\lambda 1$ and $\lambda 2$ are split into two optical paths at a second optical coupler (OC2). In the upper path where a PS-FBG is incorporated, the phase-modulated signal at $\lambda 1$ is reflected and filtered by the PS-FBG. When the upper sideband falls in the notch of the PS-FBG, the phase-modulated signal is converted to an SSB intensity-modulated signal, and the detection of the SSB intensity-modulated signal at a PD would lead to the generation of an electrical signal. The operation corresponds to a single band-pass MPF with the central frequency of the passband determined by the wavelength difference between the optical carrier at $\lambda 1$ and the sideband falling in the notch of the PS-FBG. The tunability can be achieved by tuning the wavelength of LD1, and the frequency tuning range can be as wide as tens of gigahertz, determined by the reflection bandwidth of the PS-FBG and the notch location within the reflection band, as shown in Fig. 1(b). In the lower path where an OBPF is incorporated, the phase-modulated signal at $\lambda 2$ is filtered by the OBPF, and the lower sideband is fully removed. Thus, the phase-modulated signal is also converted to an SSB intensity-modulated signal. Due to the wide bandwidth of the OBPF, an allpass filter is implemented. An optical variable delay line (OVDL) is inserted in one path to ensure the delay times of the two paths are identical. Since the remaining lower sideband for $\lambda 1$ and the upper sideband for $\lambda 2$ are out of phase, the beating between the optical carrier and the lower sideband will cancel completely the beating between the optical carrier and the upper sideband when the powers of the two beat signals are controlled identical, thus a single notch filter with a high rejection depth is realized. The notch frequency can be tuned by adjusting the wavelength of LD1. The notch rejection depth can also be tuned by controlling the power difference between the two wavelengths.

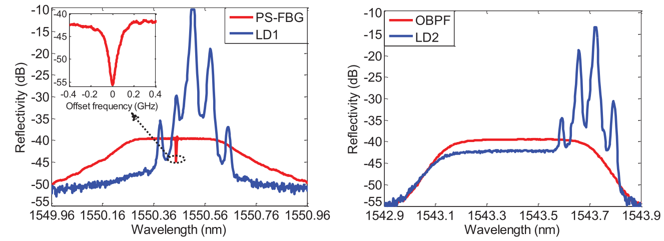

Fig. 2. The spectra of (a) the phase-modulated signal at the output of the PS-FBG, and (b) the phase-modulated signal at the output of the OBPF.

III. Experiment and Results

An experiment based on the setup shown in Fig. 1(a) is performed. Two light waves from LD1 and LD2 at about 1550.50 nm and 1543.72 nm are combined at OC1 and sent to the PM (JDS Uniphase, 20Gb/s) where the two light waves are modulated by a microwave signal from a vector network analyzer (VNA, Agilent E8364A). The insertion loss of the PM is about 5 dB. The phase-modulated signals are amplified by an erbium-doped fiberamplifier (EDFA) with a constant output power of 10 dBm, and then split into two paths by OC2, with the PS-FBG in the upper path and the OBPF in the lower path. The PS-FBG has an ultra-narrow notch with a 3-dB bandwidth of about 1.52 pm at 1550.448 nm in the middle of the reflection band, and the OBPF has a 3-dB bandwidth of about 0.6 nm with a central wavelength at 1543.40 nm. The wavelength at $\lambda 1$ is greater than the notch wavelength of the PS-FBG, and the wavelength at $\lambda 2$ is located near the right slope of the OBPF. The OVDL in the lower path is used to finely control the delay times to be equal. The two optical signals from the two paths are combined at OC3 and then sent to the PD. The frequency response is measured by the VNA.

Fig. 2(a) shows the spectra of the PS-FBG (red) and the phase-modulated signal at the output of the PS-FBG (blue). A zoom-in view of the notch is shown in the inset in Fig. 2(a). As can be seen the PS-FBG has a notch with a rejection of 14 dB and the total reflection bandwidth is about 27.5 GHz. The upper sideband is located at the notch of the PS-FBG and it is removed. Fig. 2(b) shows the spectra of the OBPF (red) and the phase-modulated signal at the output of the OBPF (blue). The lower sideband is located outside the passband and it is removed by the OBPF. For the phase-modulated signal at $\lambda 1$, the beating between the remaining lower sideband and the optical carrier would implement a single bandpass filter, as shown in Fig. 3 (red). For the phase-modulated signal at $\lambda 2$, the beating between the optical carrier and the remaining upper sideband would implement an allpass filter, as shown in Fig. 3 (blue). Since the two beat signals are out of phase, the combination of the two beat signals performs a subtraction operation, and thus a notch filter is achieved, as shown in Fig. 3 (black). To ensure a high rejection depth, the powers from the two beat signals should be controlled equal, which can be done by adjusting the powers of LD1 and LD2. As can be seen from Fig. 3, the powers for the allpass filter and the bandpass filter are equal, which ensures a deep notch. The rejection depth seen from the inset in Fig. 3 is 42 dB and the 3-dB width is about 180 MHz. The notch width can be further reduced if a PS-FBG with a narrower notch is used. From Fig. 3, it can also be seen that the insertion loss

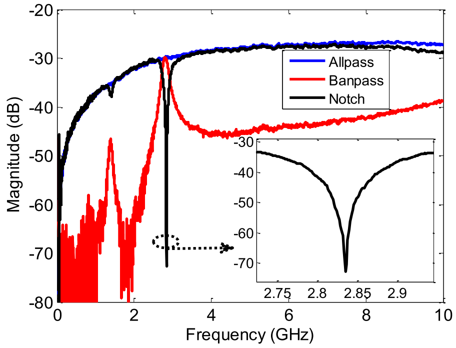

Fig. 3. Frequency responses of the allpass filter, the bandpass filter, and the corresponding notch filter.

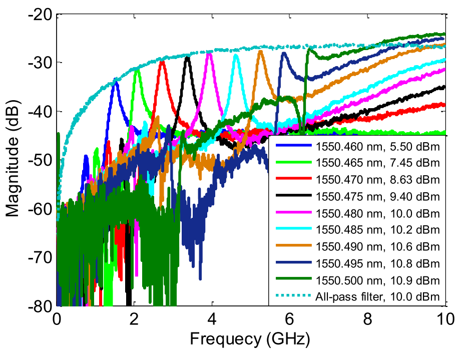

Fig. 4. Frequency response of the allpass filter and the bandpass filter with the power of the bandpass filter adjusted to match the power of the allpass filter.

is about 30 dB. Such a high insertion loss is mainly caused by the poor power handling capability of the PD (New Focus 10058B, 20 GHz). In the experiment, the average input power is about −1 dBm. By using a high-power handling PD, the insertion loss can be greatly reduced. One may note that the allpass filter has a broad notch at the lower frequencies with a 3-dB bandwidth of about 4 GHz, which is resulted from the broad transition band of approximately of 0.032 nm of the OBPF, as can be seen in Fig. 2.

Since the center frequency of the bandpass filter depends on the wavelength difference between $\lambda 1$ and the PS-FBG notch, the notch frequency of the proposed MPF can be tuned by tuning the wavelength of LD1. In the experiment, we tune the wavelength of LD1 with a tuning step of 5 pm. Fig. 4 shows the tunable frequency response of the bandpass filter and that of the allpass filter. Note that during the tuning the power at the output of the allpass filter is kept constant by setting the power of LD2 at 10 dBm and the power at the output of the bandpass filter is adjusted by changing the power of LD1 to maximize notch depth. If the bandpass power is also kept constant, the notch depth will become smaller due to the increase in the power difference. Fig. 5 shows the notch frequency response of the MPF. As can be seen a high rejection depth over the frequency tuning range is obtained. Some variations in the rejection depth from 35 to 42 dB (or 7 dB change) are observed, which are resulted from the variations of the power difference between the two channels. In fact, the 7 dB change corresponds to a power variation of only 0.025%.

On the other hand, if the power at the output of the bandpass filter is maintained constant and the power at the output of

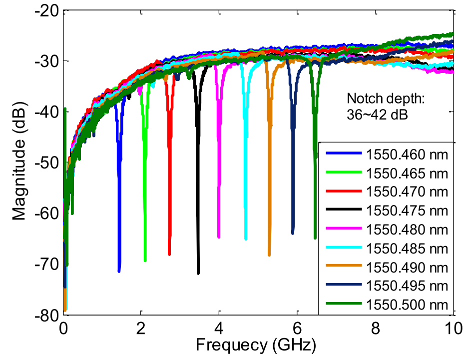

Fig. 5. Frequency response of the proposed notch filter with the allpass power kept constant and the power of the bandpass filter adjusted to match the power of the allpass filter.

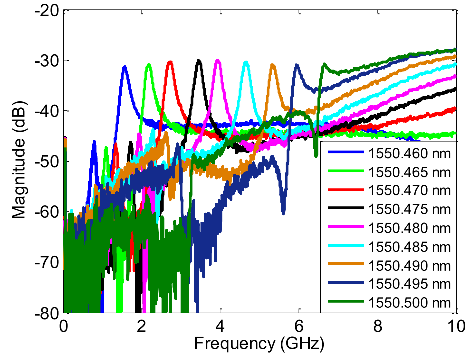

Fig. 6. Frequency response of the bandpass filter with the power kept constant.

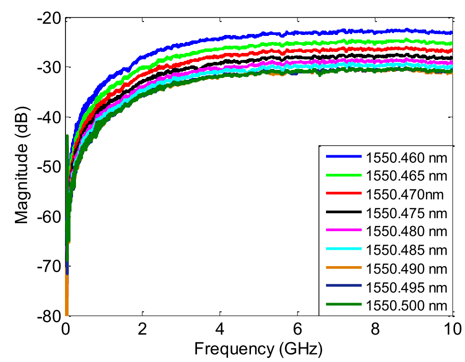

Fig. 7. Frequency response of the allpass filter with the power adjusted to match the power of the bandpass filter.

the allpass filter is adjusted, a high notch depth can also be achieved. To do so, in the experiment we set the power of LD1 at a fixed value of 10.9 dBm, and change the power of LD2 to maintain a high notch depth. Fig. 6 shows the frequency response of the bandpass filter at different frequencies for the power of LD1 at 10.9 dBm. As can be seen the power level maintains constant. Fig. 7 shows the frequency response of the allpass filter with the power tuned to match that of the bandpass filter shown in Fig. 6. As can be seen that the power difference between adjacent allpass filter becomes smaller when the wavelength of LD1 is increased, and the corresponding center frequency of the bandpass is increased.

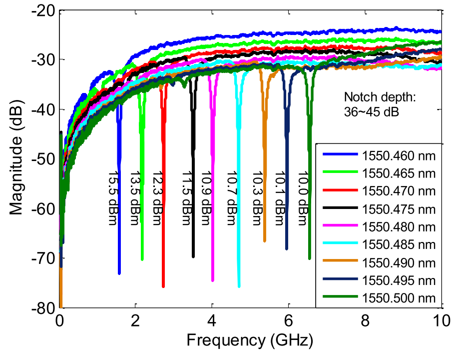

Fig. 8. Frequency response of the proposed notch filter with the bandpass power kept constant and the power of the allpass filter adjusted to match the power of the bandpass filter.

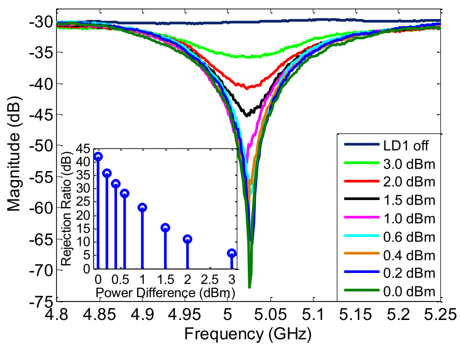

Fig. 9. Frequency response to show the tuning of the notch depth. Inset: relationship between the notch depth and the power difference.

This is because the allpass filter response has larger power variation in the low frequency region and becomes nearly constant in the high frequency region.

Fig. 8 shows the frequency response of the proposed notch filter, and the notch depth varies from 36 to 45 dB. Again, the variations in notch depth are resulted from variations of the power difference between the two channels. The variations are resulted from the environmental changes (mainly vibrations) since the system is implemented using discrete fiber-optic components in a lab environment. The power variations can be reduced if the system is well packaged or it is implemented using a photonic integrated circuit (PIC).

Note that the wavelength difference between LD1 and LD2 should be sufficiently large to avoid a beat signal generated at the output of the PD. In our experiment, the wavelength spacing is more than 6 nm, corresponding to a beat frequency of 750 GHz, which is too high to be detected by the PD.

The tunability of the notch depth is also investigated. During the tuning, the power of the allpass filter is kept constant, and the power of the bandpass filter is adjusted. Fig. 9 shows the frequency response of the proposed notch filter with different power difference by reducing the power of LD1. As can be seen a different value of the power difference results in a different notch depth. The inset in Fig. 9 shows the relationship between the notch depth and the power difference. When LD1 is turned off, the notch depth becomes zero and the filter becomes an allpass filter.

IV. Conclusion

A single-notch microwave photonic filter with both tunable frequency and tunable notch depth was proposed and experimentally demonstrated. The fundamental concept to produce a deep notch is to use the out-of-phase nature of the two sidebands of a phase-modulated signal. In the proposed MPF, two phase-modulated signals were converted to two SSB intensity-modulated signals, with one having its upper sideband removed by the PS-FBG and the other having the lower sideband removed by the OBPF. Since the remaining two sidebands in the two optical SSB signals were out of phase, the combination of the beat signals at the PD led to the cancellation of the detected microwave signals, and a notch was achieved. By controlling the power levels of the two signals at the output of the PD identical, a notch with an infinite notch depth would be resulted. The proposed filter was experimentally evaluated. A microwave notch filter with a 3-dB bandwidth of about 180 MHz and a notch depth of over 40 dB was achieved. The frequency tunability was also studied. By tuning the wavelength of LD1, an MPF with a frequency tunable range from 1.5 to 6.6 GHz was demonstrated. The tuning of the notch depth was also studied. By changing the power difference between the powers of the bandpass filter and the allpass filter, a tunable depth from 0 to 42 dB was demonstrated.

References

[1] J. Capmany and D. Novak, "Microwave photonics combines two worlds," *Nature Photon.*, vol. 1, no. 6, pp. 319–330, Jun. 2007.

[2] R. A. Minasian, "Photonic signal processing of microwave signals," *IEEE Trans. Microw. Theory Techn.*, vol. 54, no. 2, pp. 832–846, Feb. 2006.

[3] J. Capmany, J. Mora, I. Gasulla, J. Sancho, J. Lloret, and S. Sales, "Microwave photonic signal processing," *J. Lightw. Technol.*, vol. 31, no. 4, pp. 571–586, Feb. 15, 2013.

[4] J. Yao, "Microwave photonics," *J. Lightw. Technol.*, vol. 27, no. 3, pp. 314–335, Feb. 1, 2009.

[5] D. Norton, S. Johns, C. Keefer, and R. Soref, "Tunable microwave filtering using high dispersion fiber time delays," *IEEE Photon. Technol. Lett.*, vol. 6, no. 7, pp. 831–832, Jul. 1994.

[6] B. Vidal, J. L. Corral, and J. Marti, "All-optical WDM microwave filter with negative coefficients," *IEEE Photon. Technol. Lett.*, vol. 17, no. 3, pp. 666–668, Mar. 2005.

[7] D. Pastor, J. Capmany, and B. Ortega, "Broad-band tunable microwave transversal notch filter based on tunable uniform fiber Bragg gratings as slicing filters," *IEEE Photon. Technol. Lett.*, vol. 13, no. 7, pp. 726–728, Jul. 2001.

[8] R. A. Minasian, K. E. Alameh, and E. H. W. Chan, "Photonics-based interference mitigation filters," *IEEE Trans. Microw. Theory Techn.*, vol. 49, no. 10, pp. 1894–1899, Oct. 2001.

[9] E. H. W. Chan and R. A. Minasian, "High-resolution photonics-based interference suppression filter with wide passband," *J. Lightw. Technol.*, vol. 21, no. 12, pp. 3144–3149, Dec. 2003.

[10] Y. Yu, E. Xu, J. Dong, L. Zhou, X. Li, and X. Zhang, "Switchable microwave photonic filter between high *Q* bandpass filter and notch filter with flat passband based on phase modulation," *Opt. Exp.*, vol. 18, no. 24, pp. 25271–25282, Nov. 2010.

[11] W. Zhang and R. A. Minasian, "Ultrawide tunable microwave photonic notch filter based on stimulated Brillouin scattering," *IEEE Photon. Technol. Lett.*, vol. 24, no. 14, pp. 1182–1184, Jul. 15, 2012.

[12] D. Marpaung, B. Morrison, R. Pant, and B. J. Eggleton, "Frequency agile microwave photonic notch filter with anomalously high stopband rejection," *Opt. Lett.*, vol. 38, no. 21, pp. 4300–4303, Nov. 2013.

[13] D. Marpaung *et al.*, "Low-power, chip-based stimulated Brillouin scattering microwave photonic filter with ultrahigh selectivity," *Optica*, vol. 2, no. 2, pp. 76–83, Feb. 2015.